Journal of the Korea Concrete Institute
Vol.18 No.1, pp.135~145, February, 2006

The Steel Coupling Beam-Wall Connections Strength

Wan-Shin Park[1] and Hyun-Do Yun[2]*

[1]*Dept. of Civil and Environmental Engineering, University of Cincinnati, Ohio, USA*
[2]*Dept. of Architectural Engineering, Chungnam National University, Daejeon 305-764, Korea*

(Received February 24, 2005, Accepted December 30, 2005)

Abstract

In high multistory reinforced concrete buildings, coupled shear walls can provide an efficient structural system to resist horizontal force due to wind and seismic effects. Coupled shear walls are usually built over the whole height of the building and re laid out either as a series of walls coupled by beams and/or slabs or a central core structure with openings to accommodate doors, elevators walls, windows and corridors. A number of recent studies have focused on examining the seismic response of concrete, steel, and composite coupling beams. However, since no specific equations are available for computing the bearing strength of steel coupling beam-wall connections, it is necessary to develop such strength equations. There were carried out analytical and experimental studies to develop the strength equations of steel coupling beam-connections. Experiments were conducted to determine the factors influencing the bearing strength of the steel coupling beam-wall connection. The results of the proposed equations were in good agreement with both test results and other test data from the literature. Finally, this paper provides background for design guidelines that include a design model to calculate the bearing strength of steel coupling beam-wall connections.

Keywords* : *steel coupling beams, connection strength, stud bolts

1. Introduction

Properly designed coupled walls have many desirable earthquake-resistant design features. Large lateral stiffness and strength can be achieved. By coupling beam individual flexural walls, the lateral load resisting behavior changes to on where overturning moments are resisted partially by an axial compression-tension couple across the wall system rather than by the individual flexural action of the walls. The beams that connect individual wall piers are referred to as coupling beams. In order for the desired behavior of the hybrid wall system to be attained, the coupling beams, however, must also yield before the wall piers, behave in a ductile manner, and exhibit significant energy absorbing characteristics.

Several researchers have investigated novel approaches to improve the ductility and energy absorption of reinforced concrete coupling beams. A coordinated experimental research programs at the University of Cincinnati in USA[1] has examined the cyclic response of steel coupling beam and the overall behavior of hybrid coupled shear wall systems. Testing of hybrid coupled shear wall systems at the University of McGill in Canada[2] led to recommendations for designing steel coupling beams in hybrid coupled shear wall systems. Experimental and numerical studies on concrete-steel composite coupling beam at the University of Hong Kong in China[3] were conducted to investigate the effects of encasement around shear-yielding steel coupling beams. These experimental studies were primarily concerned with the inelastic cyclic behavior of steel coupling beams or hybrid coupled shear wall systems and did not deeply investigate connection strength. The experimental studies on the steel coupling beams in a hybrid coupled shear walls at the Chungnam National University in Republic of Korea[4] investigated the seismic behavior of steel coupling beams considering connection details. As mentioned above, a number of recent studies have focused on examining the seismic response of concrete, steel, and composite coupling beams. However, since no specific equations are available for computing the bearing strength

* *Corresponding author*
Email address: wiseroad@cnu.ac.kr
©2006 by Korea Concrete Institute

of connection between steel coupling beam and reinforced concrete shear wall, it is necessary to develop such strength equations.

In this study, it were set out to develop the strength equations of connection between steel coupling beam and reinforced concrete shear wall in a hybrid wall system, and analytical and experimental studies on joint of steel coupling beam-concrete shear wall were carried out. Each specimen consisted of a wall pier and a steel beam embedded in the wall to represent a steel coupling beam, and the test results are discussed later on. Governed by the bearing on the concrete, the experimental results of specimens subjected to reverse cyclical loading were used to revise and verify the proposed strength equation capacities of connection between steel coupling beam and reinforced concrete shear wall.

2. Code provision and existing model

Since the coupling beam is expected to undergo significant inelastic deformation, then its embedment must be capable of developing forces corresponding to the plastic capacity of the beam. No specific guidelines are available for computing the bearing strength of connection between steel coupling beam and reinforced concrete shear wall, but references to previous studies show the adequacy of four models proposed by the Prestressed Concrete Institute (PCI), Chicago, USA[5,6], Kriz and Raths[7], Williams[8], and Mattock and Gaafar[9]. These four models were originally developed for the design of precast, bracket, corbel, and beam-column joint, respectively, and have been used to propose equations describing the strength of connection between steel coupling beam and reinforced concrete shear wall.

Design equations based on conservative simplifying assumptions have been developed by the PCI Committee[5,6] on joint details for embedded steel coupling beam sections. A defined concrete force system was assumed at the ultimate strength, as shown in Fig. 1. By taking moments about the line of action at point C_b, the following equation is obtained

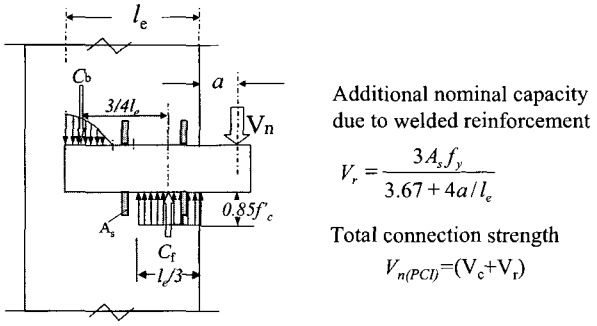

Fig. 1 Concrete force system at ultimate load assumed by PCI committee

$$V_c = \frac{0.85 f_c' \beta_1 b l_e}{(3.67 + 4a/l_e)} \quad \text{(N)} \tag{1a}$$

The additional capacity due to the auxiliary bars can be computed using equation (1b)

$$V_r = \frac{3A_s f_y}{(3.67 + 4a/l_e)} \quad \text{(N)} \tag{1b}$$

and

$$V_{n(PCI)} = (V_c + V_r) \quad \text{(N)} \tag{1c}$$

Kriz and Raths[7] suggested that the concrete bearing stress was proportional to $\sqrt{f_c'}$, and proposed equations of the following form for the joint of precast concrete structures

$$V_{n(Kriz\ \&\ Raths)} = 5.7\sqrt{f_c'}\beta_1 b l_e \left(\frac{t/2}{b}\right)^{0.33} \left(\frac{0.58 - 0.22\beta_1}{0.88 + a/l_e}\right) \quad \text{(N)} \tag{2}$$

In addition, the following equation was proposed by Williams[8]

$$V_{n(Williams)} = 5.7\sqrt{f_c'}\beta_1 b l_e \left(\frac{t/2}{b}\right)^{0.47} \left(\frac{0.58 - 0.22\beta_1}{0.88 + a/l_e}\right) \quad \text{(N)} \tag{3}$$

To facilitate the design calculations, Mattock and Gaafar[9] proposed the following equations for steel brackets.

$$V_{n(Mattcok)} = \frac{1.75\sqrt{t/b}\sqrt{f_c'} b l_e}{0.88 + a/l_e} \quad \text{(N)} \tag{4}$$

The experimental results[9-13] of steel bracket, precast, steel beam-concrete column joint, and coupled shear walls have been used to propose the strength equations of connection between steel coupling beam and reinforced concrete shear wall. As can be seen from Table 1, these parameters include the width of the steel beams, the embedment length, the thickness of the wall(or width of the column), the distance from the concentrated load to the face of the wall(or column), and the concrete compressive strength. As shown in Fig. 2(a), the observed values ranged from 1.2 to 4.5 times those predicted by PCI Code. As shown in Figs. 2(b) and 2(c), the observed values ranged from 0.82 to 2.38

times those predicted by Kriz and Raths[7] and by Williams[8]. In addition, as shown in Fig. 2(d), the observed values ranged from 0.79 to 1.83 times those predicted by Mattock and Gaafar[9].

As mentioned above, the existing models are very conservative. This can be attributed to the assumed size of the

Table 1 Comparison with other test data

Researcher	Specimen Name	b (mm)	b_{eff} (mm)	c (mm)	l (mm)	l_e (mm)	l_v (mm)	l_{eff} (mm)	t (mm)	a (mm)	f_{cu} (MPa)	b/t (-)	e (mm)	Section (mm)	$V_{n(test)}$ (kN)
Mattock & Gaafar[9] (1982)	R2	50.8	-	38.1	-	254	-	-	254	102	27.8	0.20	-	4.45×2	247.0
	R5	127.0	-	38.1	-	254	-	-	254	102	28.3	0.50	-	3.24×5	340.1
	I3	76.2	-	38.1	-	254	-	-	254	102	26.6	0.30	-	H-101×76×25×25	298.2
	I3F	76.2	-	38.1	-	254	-	-	254	102	27.5	0.30	-	H-101×76×25×25	233.6
	W4	101.6	-	38.1	-	203	-	-	254	152	20.3	0.40	-	H-152×101×58×71	169.1
Clarke & Symmons[10] (1978)	B1(3)	38	-	40	-	125	150	-	145	50	33.0	0.26	-	38×38	90.0
	B2(1)	51	-	40	-	125	150	-	150	50	23.2	0.34	-	51×51	85.0
	B2(2)	51	-	40	-	125	150	-	150	50	23.2	0.34	-	51×51	80.0
	B2(3)	51	-	40	-	125	150	-	150	50	16.6	0.34	-	51×51	56.0
	B3(1)	51	-	40	-	125	150	-	150	50	20.9	0.34	-	51×38	62.0
	B3(2)	51	-	40	-	125	150	-	150	50	20.9	0.34	-	51×38	60.0
	B3(3)	51	-	40	-	125	150	-	150	50	20.9	0.34	-	51×38	67.0
	B4(1)	76	-	40	-	125	150	-	150	50	23.2	0.51	-	76×51	91.0
	B4(2)	76	-	40	-	125	150	-	150	50	16.6	0.51	-	76×51	80.0
	B4(3)	76	-	40	-	125	150	-	150	50	16.6	0.51	-	76×51	70.0
	C2(1)	51	-	40	-	125	150	-	150	50	16.6	0.34	-	51×51	66.0
	C2(2)	51	-	40	-	125	150	-	150	50	16.6	0.34	-	51×51	68.0
	C2(3)	51	-	40	-	125	150	-	150	50	16.6	0.34	-	51×51	77.0
	C3(1)	51	-	40	-	125	150	-	149	50	29.0	0.34	-	51×38	90.0
	C3(2)	51	-	40	-	125	150	-	149	50	29.0	0.34	-	51×38	90.0
	C3(3)	51	-	40	-	125	150	-	149	50	29.0	0.34	-	51×38	90.0
	C4(1)	76	-	40	-	125	150	-	150	50	20.8	0.51	-	76×51	92.0
	C4(2)	76	-	40	-	125	150	-	150	50	16.6	0.51	-	76×51	72.0
	C4(3)	76	-	40	-	125	150	-	147	50	30.6	0.52	-	76×51	124.0
	D1(1)	38	-	40	-	125	150	-	150	50	26.5	0.25	-	38×38	80.0
	D1(2)	38	-	40	-	125	150	-	150	50	26.5	0.25	-	38×38	80.0
	D1(3)	38	-	40	-	125	150	-	150	50	26.5	0.25	-	38×38	80.0
	D2(1)	51	-	40	-	125	150	-	150	50	20.8	0.34	-	51×51	84.0
	D2(2)	51	-	40	-	125	150	-	150	50	16.6	0.34	-	51×51	71.0
	D2(3)	51	-	40	-	125	150	-	150	50	16.6	0.34	-	51×52	74.0
	D3(1)	51	-	40	-	125	150	-	150	50	21.6	0.34	-	51×38	93.0
	D3(2)	51	-	40	-	125	150	-	150	50	21.6	0.34	-	51×38	97.0
	D3(3)	51	-	40	-	125	150	-	150	50	21.6	0.34	-	51×38	94.0
	D4(1)	76	-	40	-	125	150	-	150	50	26.6	0.51	-	76×51	130.0
Marcakis & Mitchell[11] (1980)	C1	101.6	-	40	-	152	-	-	178	76	33.1	0.57	-	4×4×1/4 tube*	123.7
	C2	101.6	-	40	-	152	-	-	178	76	26.9	0.57	-	4×4×1/4 tube#	184.2
	C3	101.6	-	40	-	152	-	-	178	76	35.9	0.57	-	4×4×1/4 tube#	200.2
	C4	101.6	-	40	-	152	-	-	178	76	40.0	0.57	-	4×4×1/4 tube#	238.0
	SC2	101.6	-	40	-	178	-	-	203	76	31.0	0.50	-	6×4×3/2 tube#	244.7
	SC3	101.6	-	40	-	178	-	-	203	102	31.0	0.50	-	6×4×3/2 tube#	314.5
	SC4	101.6	-	40	-	178	-	-	203	102	31.0	0.50	-	6×4×3/2 tube#	297.1
	SC5	101.6	-	40	-	178	-	-	203	102	31.0	0.50	-	6×4×3/2 tube#	244.7
	SC6	101.6	-	40	-	178	-	-	203	102	31.0	0.50	-	W6in×25lb$	270.9
	SC9	101.6	-	40	-	178	-	-	184	111	31.0	0.55	-	6×4×3/8 tube#	218.4
	SC10	101.6	-	40	-	194	-	-	254	76	31.0	0.40	-	6×4×3/8 tube#	279.3
	TC1	101.6	-	40	-	184	-	-	406	102	23.4	0.25	-	4×4 solid bar	262.0
	PL1	19.05	-	40	-	102	-	-	203	76	47.6	0.09	-	3/4×4 plate	87.2
Bahram M. Shahrooz[12] (1993)	W1	203.0	254.0	40.0	434.0	229	-	189	254	267	35.0	0.80	352	H-457×203×25×25	246.9
Kent Harries[13] (1995)	S1	135.0	200.0	40.0	1200.0	600	-	560	300	600	25.9	0.45	920	H-347×135×5×19	303.0

* Tube empty
\# Tube filled with concrete
$ Flanges cut to 4in. wide

concrete compression zone below the embedded steel section, the size of the internal lever arm between points C_b and C_f, and the correctness of the assumed effective width, b, of the embedded steel section. In addition, the contribution of the auxiliary bars and the horizontal bars are not considered in current models. Therefore, it were set out to obtain a better understanding of the behavior and the bearing strength of connection between steel coupling beam and reinforced concrete shear wall.

3. Analytical Study

3.1 Bearing strength of concrete above and below the embedded steel section

Fig. 3 shows actual and assumed stresses and strains for connection between steel coupling beam and reinforced concrete shear wall. The compressive stresses in the concrete above and below the embedded steel section caused by the load, V_n, acting on the section at a given distance from the face of the concrete shear walls are shown in Fig. 3(a). The applied shear (V_n) is resisted by mobilizing an internal moment arm between the bearing forces, C_f and C_b.

For calculation purposes, the stresses in the concrete at the ultimate stress are assumed to be as shown in Fig. 3(b). The parabolic compressive stress distribution below the embedded steel coupling beam section has been replaced by the equivalent rectangular stress distribution, equal to $0.85f_{ck}$, which is defined in Section 10.2.7 of the ACI 318-05 report[14]. The parabolic distribution of bearing stresses

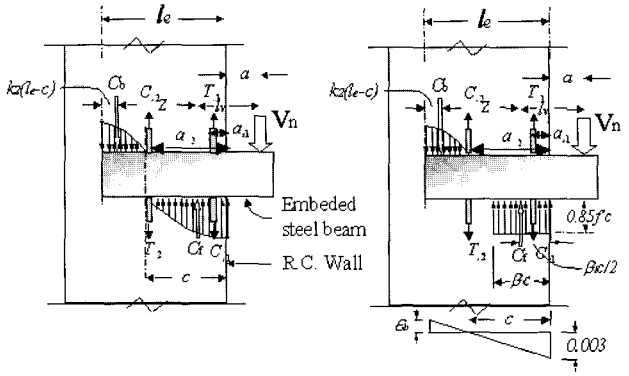

(a) Actual stresses (b) Assumed stresses and strain

Fig. 3 Actual and assumed stresses and strains in concrete adjacent to embedded steel coupling beam section

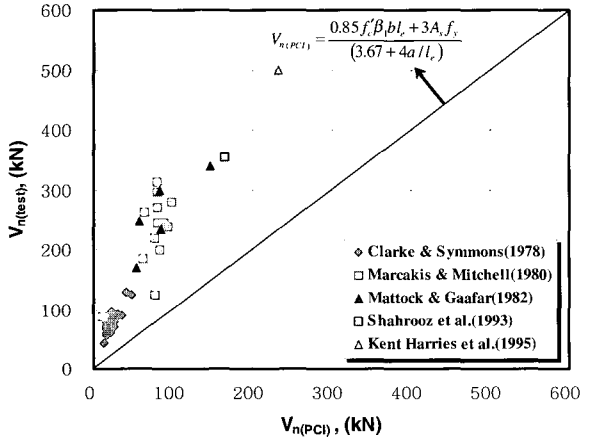

(a) Comparison of predicted values by PCI Code and observed strength

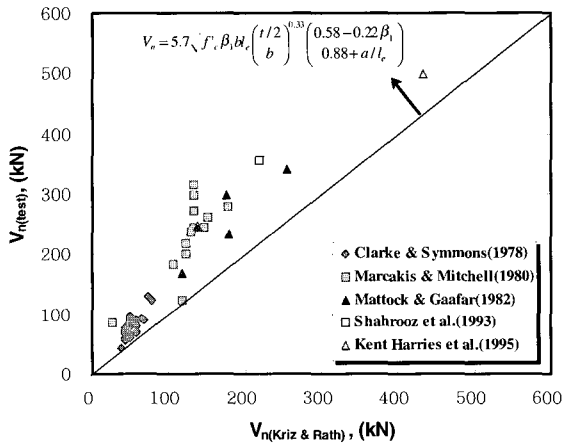

(b) Comparison of values predicted by Kriz and observed strength

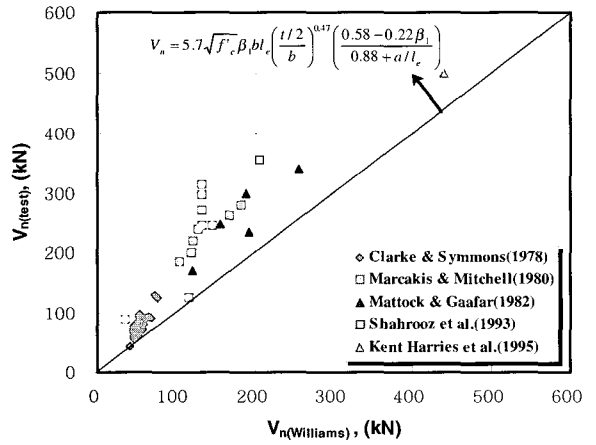

(c) Comparison of predicted values by Williams and observed strength

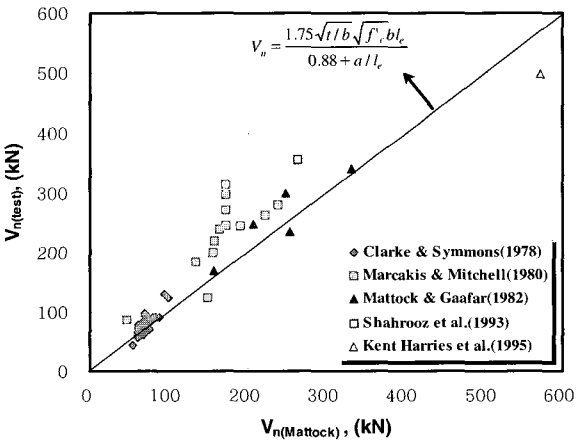

(d) Comparison of values predicted by Mattock and observed strength

Fig. 2 Comparison of values predicted by PCI Code and previously proposed Eq. and observed strength

above the embedded steel coupling beam section is assumed to obey the following stress-strain relationship proposed by Kent and Park[15].

$$f_c = f_{ck}\left[\frac{2\varepsilon_c}{0.002} - \left(\frac{\varepsilon_c}{0.002}\right)^2\right] \text{ (MPa)} \quad (5)$$

and is also assumed that there is a linear relationship between the compressive strains above and below the steel coupling beam section, as shown in Fig. 3(b). The assumed stress-strain relationship for concrete above the embedded steel coupling beam section corresponds to a parabola with a maximum stress of f_{ck} at a strain = 0.002. The factor, k_2, defining the location of the resultant compressive force, C_b, is given by

$$k_2 = \left[\frac{1-0.375\left(\frac{l_e-c}{c}\right)}{3-1.50\left(\frac{l_e-c}{c}\right)}\right] \quad (6)$$

Therefore, V_n may be obtained by taking moments about the line of action at point C_b, as

$$V_n = 0.85 f_{ck}\beta_1 b l_e\left(\frac{c}{l_e}\right)\left[\frac{1-k_2\left(1-\frac{c}{l_e}\right)-\frac{\beta_1}{2}\left(\frac{c}{l_e}\right)}{1-k_2\left(1-\frac{c}{l_e}\right)+\frac{a}{l_e}}\right] \quad (7)$$

The value of c/l_e was corresponded to the values of a/l_e = 0.5–2.7 for 20.7< f_{ck} /MPa < 55.2, i.e., for β_1 = 0.85–0.79.

Fig. 4 shows that the value of c/l_e has only a small variation from its average value. As shown in Fig. 4, the average value of c/l_e was 0.66, and the coefficient of variation was 3.5% for normal-strength concrete. Therefore, the value of c/l_e was assumed to be c/l_e = 0.66. It follows from equation (6) that k_2 = 0.36. Then, $V_{n(theory)}$ is given by

$$V_{n(theory)} = 0.85 f_{ck}\beta_1 b l_e\left(\frac{c}{l_e}\right)\left[\frac{0.58-0.22\beta_1}{0.88+a/l_e}\right] \text{ (N)} \quad (8)$$

The flange width was assumed to be fully effective in developing the bearing stresses. Based on these assumptions, and by calibrating using experimental data obtained from steel bracket, precast, corbel, and steel beam-concrete column joint subjected to cyclic loading, the embedment

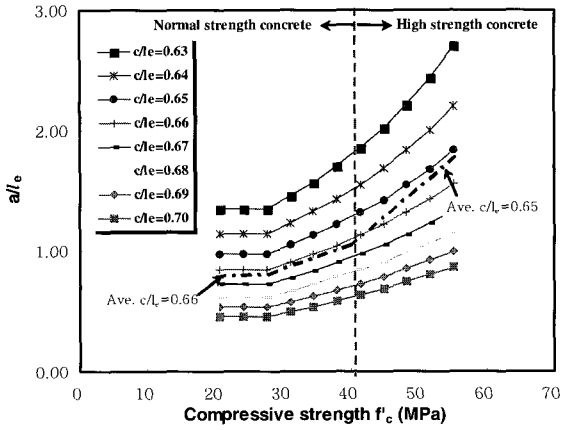

Fig. 4 c/l_e versus concrete compressive strength and a/l_e

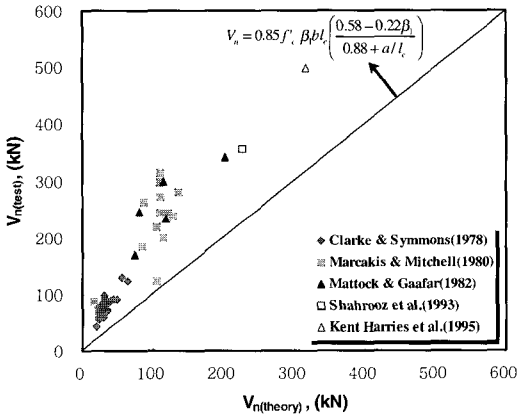

Fig. 5 Comparison of values predicted by theoretical Eq. and observed strength

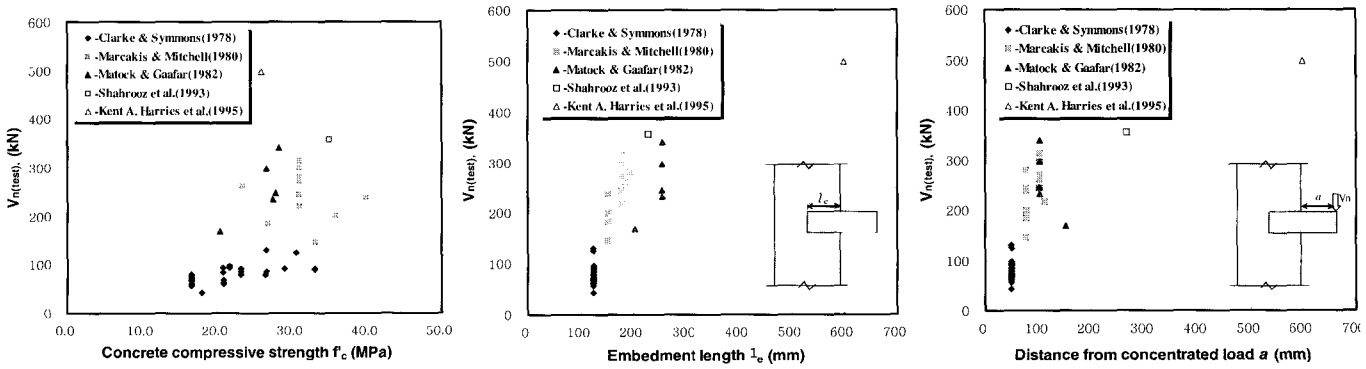

(a) Influence of the concrete compressive strength (b) Influence of the embedment length (c) Influence of the distance from concentrated load

Fig. 6 Evaluations of influential factors

length of the steel coupling beam was computed using equation (8). Fig. 5 shows comparisons between the predicted values from the theoretical equations and the observed strength. As shown in Fig. 5, the predicted values from the theoretical equations underestimate the observed strength.

3.2 Evaluations of influential factors

Fig. 6 shows a graph of the bearing strength versus the concrete compressive strength, embedment length, and the distance from the concentrated load to the face of the shear wall or column.

The bearing strength of the connection between steel coupling beam and reinforced concrete shear wall increases as the concrete compressive strength increases, as shown in Fig. 6(a). This trend exhibits a shape closer to a parabolic relationship rather than a linear relationship. Fig. 6(b) shows that the bearing strength of the connection between steel coupling beam and reinforced concrete shear wall increases as the concrete embedment length increases. In addition, the bearing strength of connection between steel coupling beam and reinforced concrete shear wall decreases as the distance from the concentrated load to the face of the shear wall or column increases for $a \leq 20$, as shown in Fig. 6(c). However, since bearing failure is transformed into flexural failure with increasing distance, the bearing strength of joint between steel coupling beam and concrete shear wall is controlled by flexural moment rather than by shear force.

3.3 Contributions of auxiliary bars

Based on the test results from a previous study[16], stud bolts on the top and bottom flange of an embedded steel coupling beam section, as shown in Fig. 3, were specified in an effort to improve the stiffness, and to improve the transfer of the flange bearing force to the surrounding concrete. By taking moments about the line of action, C_b, the additional strength due to the internal moment arm among the stud bolts can be computed by using equation (9)

$$V_s = \frac{2(0.88 - a/l_e)\sum_{i=1}^{n} A_{si} f_{si}}{0.88 + a/l_e} \quad \text{(N)} \qquad (9)$$

A previous study[17] suggests that the longitudinal bars do not typically yield, and hence, the contribution of these bars to joint strength is nominal. Concrete can be confined by horizontal ties, commonly in the form of closely spaced tie reinforcements in the connection region.

Table 2 Variables of test specimens

Specimens \ Item	Stud bolts	Wall reinforcements		Eccentricity e(mm)
		In wall	In connections	
SCB-ST	None	HD13@230	HD13@230	+150
SCB-SB	12-ϕ19	HD13@230	HD13@230	+150

Table 3 Average concrete compressive strengths

Specimens \ Item	Compressive strength (MPa)	Ultimate strain ε_{cu} ($\times 10^{-6}$)	Slump (mm)	Elastic modulus (GPa)	Poisson's Ratio
SCB Series	34.0	2,340	145	26.2	0.16

* At the time of testing

Table 4 Properties of reinforcement bars and steel

Specimens \ Item		Yield strength f_y (MPa)	Yield strain ε_y ($\times 10^{-6}$)	Elastic modulus E_s(GPa)	Ultimate strength f_{su} (MPa)
Reinforcement	10mm diameter deformed bar	398	2,023	196.5	566
	13mm diameter deformed bar	400	2,033	196.8	555
Steel	Beam web	339	1,682	201.2	461
	Beam flange	352	1,827	192.7	489
Stud bolts	19mm diameter deformed bar	442	2,218	199.3	600

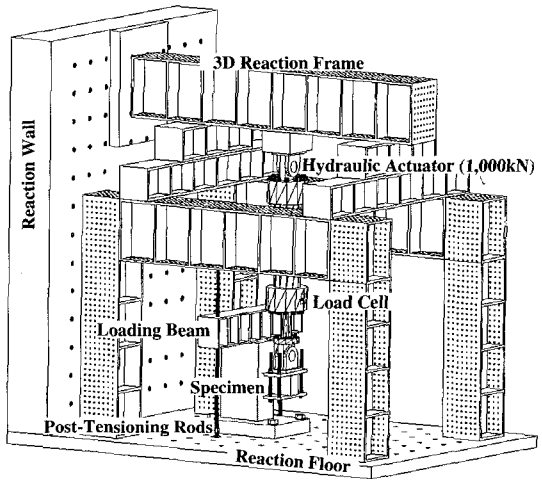

Fig. 7 Test setup

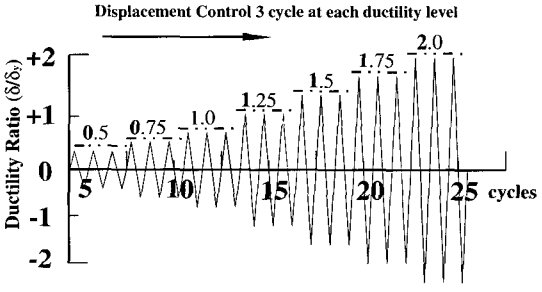

Fig. 8 Loading history

4. Experimental program

Two test specimens were employed, included on wall pier with the other two being steel coupling beams. The test subassemblages were used to review the factors influencing the bearing strength of connection between steel coupling beam and reinforced concrete shear wall. The test variables used are summarized in Table 2. The specimens were cast vertically, but typical construction joints in the wall around the connection were not reproduced. Ready-mix concrete with a minimum specified 28-day compressive strength of 34.0 MPa was used for each of the two specimens. The maximum size of concrete aggregate was 15 mm to ensure good compaction of the concrete in the test specimens.

The slump of the concrete was 145mm. For each batch, 150 x 300 mm cylinders were constructed to measure the compressive strength of the concrete. The measured concrete strength and the elastic modulus were tested using the method defined in the ASTM standards. The horizontal and vertical reinforcement consisted of ϕ=13 mm deformable bars. The reinforcing steel used for all the walls was obtained from a single batch of steel for each bar diameter, and two specimens were tested from each diameter of reinforcing used. Tension tests were conducted on full-sized bar specimens in accordance with ASTM Standard A370 to determine the yield strength, ultimate strength, and total elongation. The observed material properties are reported in Tables 3 and 4.

The data acquisition system used are consisted of 36 internal controls and recording channels. Instrumentation was provided to measure the load, displacement, and strain at critical locations. The displacement of each specimen was measured using Linear Variable Differential Transducers (LVDTs). The vertical displacement profile of each specimen was measured using LVDTs at three locations over the span of the steel coupling beams. A schematic diagram of the test apparatus is shown in Fig. 7. The test specimens were loaded using two hydraulic jacks: a pair of 2,000 kN hydraulic jack for the wall, and a 1,000 kN hydraulic jack for the steel coupling beams. The wall loading is applied

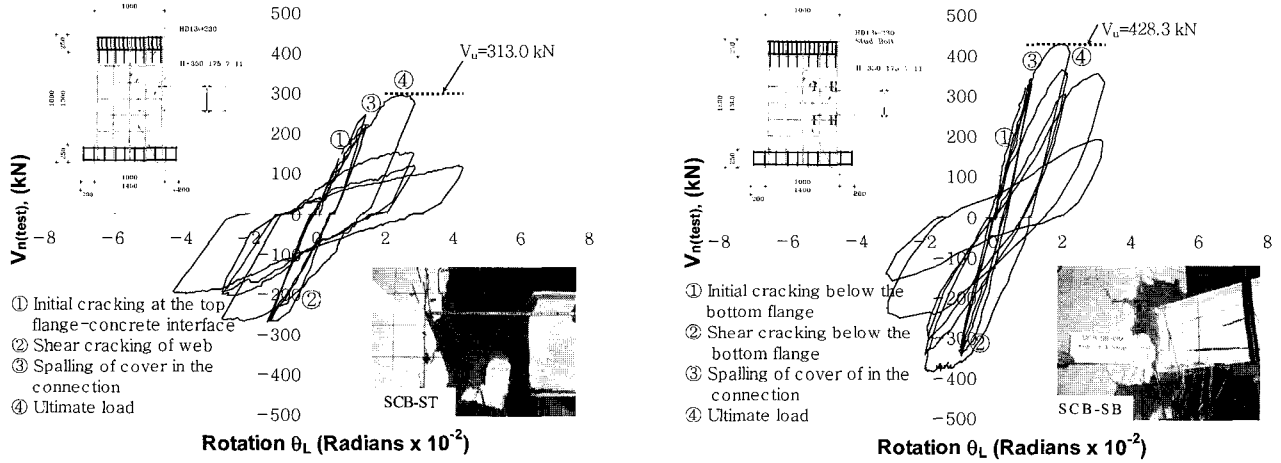

(a) SCB-ST (b) SB-SB

Fig. 9 Load versus beam rotation angle hysteretic response

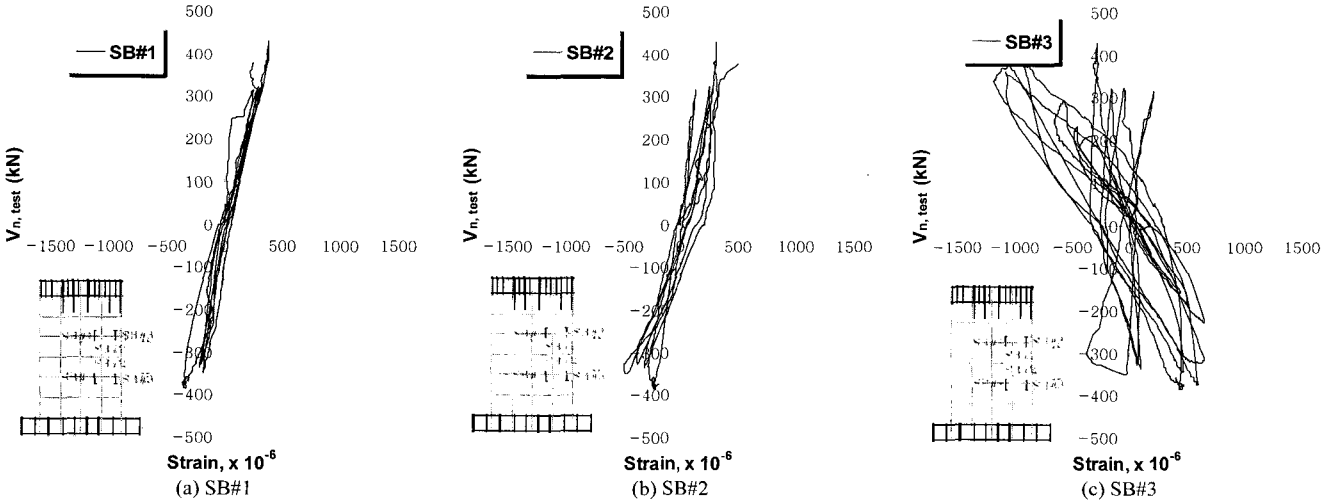

(a) SB#1 (b) SB#2 (c) SB#3

Fig. 10 Strain of stud bolts at ultimate load; Specimen SCB-SB

with tension rods and hydraulic jack located beneath the reaction floor. The displacement of all the specimens was controlled to follow similar displacement histories with progressively increasing amplitude. The observed displacement history during the tests is shown in Fig. 8; δ_y indicates the yielding displacement of the coupling beams. The data were acquired from the load on the hydraulic jacks, the deflection and rotation of the steel coupling beams, the strain in the longitudinal reinforcing bars and stud bolts in the embedment region, and strain on the flanges and web of the steel coupling beams.

4.1 Experimental results

All the specimens experienced similar damage patterns, consisting of cracking and spalling between the top and bottom flanges, as shown in Fig. 9. For all the specimens, an initial cracking at the steel coupling beam flange-concrete interface was observed during load stage 1, corresponding to a load of about ± $0.5\delta_y$. On completion of the tests, cracks with a width of up to 3 mm around the top and bottom flanges could be observed. These cracks were approximately 40 mm deep, as shown in Figs. 9(a)–10(c). Finally, spalling of the concrete below the embedded steel coupling beam section began at a load of about 92% of the ultimate load for all the specimens. Figure 9 shows a plot of the applied load versus the steel coupling beam-rotation angle. The bearing strengths of Specimens SCB-ST and SCB-SB could develop a bearing force 313 and 428.3 kN, respectively, in the compression cycles (beam push down). In particular, in specimen SCB-ST, the steel coupling beam did not reach the plastic moment capacity, because of wall spalling and bearing failure. As shown in Fig. 10, in specimen SCB-SB, the average strain of the stud bolts on the top and bottom flanges at the ultimate load was equal to about 0.000366, 0.000496, and 0.000903 for the two specimens studied. Specimen SCB-SB was reinforced by stud bolts on the top and bottom flanges, and this increased the bearing strength compared with that of specimen SCB-ST by approximately 36.7%.

Table 5 Test results

Specimens	a (mm)	l_e (mm)	f_{cu} (MPa)	$V_{n(test)}$ (kN)	$V_{n(PCI)}$ (kN)	$\frac{V_{n(test)}}{V_{n(PCI)}}$	$V_{n(theory)}$ (kN)	$\frac{(V_{test})_n}{(V_{cosub})_n}$	$\frac{f_b}{f_{cu}}$	Failure mode
SCB-ST	600	374	34.0	313.0	190.9	1.64	258.9	1.21	1.03	BF*
SCB-SB	600	374	34.0	428.3	256.9	1.66	258.9	1.65	1.41	BF

* Bearing failure
1mm=0.03937in.
1MPa=145.14psi.
1kN=0.2248kip.

4.2 Revision of the influential factors

4.2.1 Bearing stress

The maximum loads carried by the specimens are listed as the values of $V_{n(test)}$ in Table 5. Also listed in this table are the calculated ultimate loads: $V_{n(PCI)}$, using the PCI equation, and $V_{n(theory)}$ using equation (8) developed in this study. Both equations yield over-conservative estimates of the ultimate strengths of the specimens. The values from the PCI equation are about 40% more conservative than those determined using equation (8). The degree of conservatism of equation (8) increases as the width of the embedded steel coupling beam section decreases. This increase in conservatism must be due to an increase in the concrete bearing stress as the ratio of the width of the embedded steel coupling beam, b, to the thickness of the shear wall decreases. Similar behavior has been found in tests on column heads subjected to strip loading [4-6].

The ultimate strength is proportional to the bearing stress, f_b, that was assumed to be equal to $0.85f_{ck}$ when calculating $V_{n(theory)}$. Therefore, we can write

$$V_{n(test)} / f_b = V_{n(theory)} / 0.85 f_{ck} \tag{10}$$

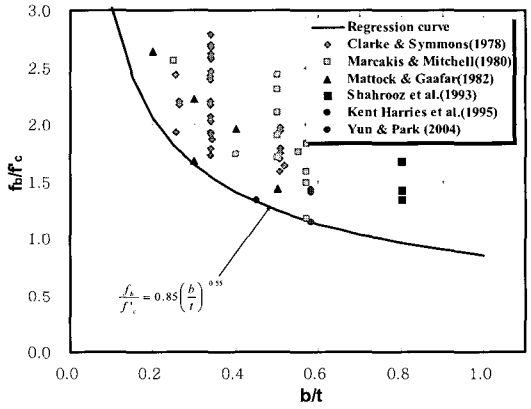

Fig. 11 Variation of bearing stress at ultimate load with ratio b/t

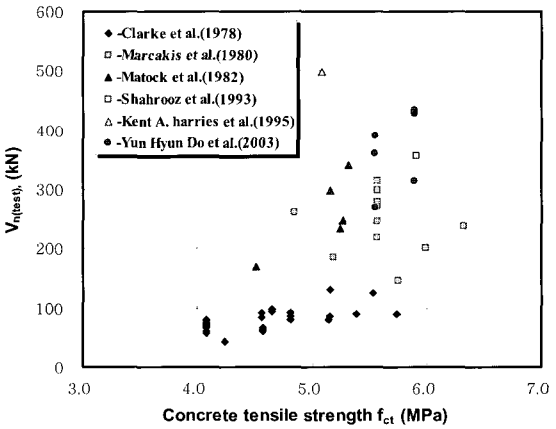

Fig. 12 Revision of influential factors

$$f_b / f_{ck} = 0.85 V_{n(test)} / V_{n(theory)} \quad (11)$$

The values of f_b / f_{ck} calculated using equation (11) are given in Table 5. The values of f_b / f_{ck} for specimens SCB-ST, SCB-SB, SCB-SBVRT, and other test data (for which the bearing width, b, is the width of the steel coupling beams) are plotted against the ratio of b/t in Fig. 11, where t is the thickness of the shear walls (or width of column). A point corresponding to the case where f_b / f_{ck} is equal to 0.85 when b/t is unity is also plotted, *i.e.*, a bearing on the full thickness of the shear walls. For a member without any horizontal ties, it can be seen that the variation of f_b / f_{ck} with b/t can be represented closely by

$$f_b / f_{ck} = 0.85\left(\frac{b}{t}\right)^{-0.55} \quad (12)$$

or

$$f_b = 28.9\left(\frac{b}{t}\right)^{-0.55} \text{ (MPa)} \quad (13)$$

for this group of specimens with an average value of $f_{ck} = 34.0$ MPa.

4.2.2 Tensile stress

The studies in References 7 and 8 found that the concrete bearing strength under strip loading was proportional to the concrete tensile strength, f_{ct}, rather than to the compressive strength, f_{ck}. The authors of References 7 and 8 assumed that f_{ct} was proportional to $\sqrt{f_{ck}}$ and proposed equations of the following form, as shown in Fig. 12

$$f_b = A\sqrt{f_{ck}}\left(\frac{t/2}{b}\right)^n \text{ (MPa)} \quad (14)$$

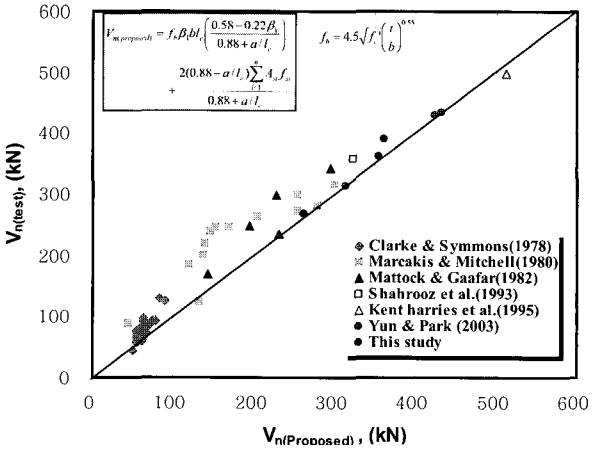

Fig. 13 Comparison of predicted values by proposed equation and observed strength

$$f_b = K\sqrt{f_{ck}}\left(\frac{t}{b}\right)^n \text{ (MPa)} \quad (15)$$

where b is the width of the steel coupling beam.

Kriz and Raths[7] proposed values of $A = 5.7$ and $n = 0.33$, *i.e.*, $K = A/2^n = 4.5$, and Hawkins[19] suggested that for design purposes, the values of A and n proposed by Kriz and Raths[7] should be used. Williams proposed a value of $n = 0.47$. In view of the findings shown in References[7] and[8], we proposed that the bearing stress below embedded sections at ultimate load be expressed in the same form as equation (15).

For member without horizontal ties, by comparing equations (13) and (15), $n = 0.55$ and $K\sqrt{f_{ck}} = 28.9$ MPa when $f_{ck} = 34.0$ MPa . Hence, the value of $K = 4.9$, which is very close to the value of A determined by Kriz and Raths[7]. Substituting the value of $K = 4.5$ proposed by Kriz and Raths[7] into equation (15), the bearing strength of concrete for an embedded steel coupling beam section without horizontal ties can be calculated using

$$V_{n(revised)} = f_b \beta_1 b l_e \left(\frac{0.58 - 0.22\beta_1}{0.88 + a/l_e}\right) \text{ (N)} \quad (16)$$

$$f_b = 4.5\sqrt{f_{ck}}\left(\frac{t}{b}\right)^{0.55} \text{ (MPa)} \quad (17)$$

Until further test data are available, it is proposed that value of the ratio of t/b not be $t/b > 2.2$ when using equations (17).

5. Proposal of strength equation

As governed by the bearings on the concrete, we proposed that the bearing strength of connection between steel coupling beam and reinforced concrete shear wall can be calculated using the following equation

$$V_{n(proposed)} = f_b \beta_1 b l_e \left(\frac{0.58 - 0.22\beta_1}{0.88 + a/l_e}\right) + \frac{2(0.88 - a/l_e)\sum_{i=1}^{n} A_{si} f_{si}}{0.88 + a/l_e} \text{ (N)} \quad (18)$$

For a member without horizontal ties

$$f_b = 4.5\sqrt{f_{ck}}\left(\frac{t}{b}\right)^{0.55} \text{ (MPa)} \quad (19)$$

where β_1 is the ratio of the depth equivalent rectangular stress distribution to the depth of flexural compression zone

as specified in Section 10.2.7 of ACI 318-05, A_{si} is cross-sectional area of the auxiliary bar, i, inside the joint, and f_{si} is the stud stresses in the auxiliary bar, i, inside the joint.

Fig. 13 shows a comparison of the experimental and predicted data from the proposed equations for the connection between steel coupling beam and reinforced concrete shear wall. When proposed equation (16) was used to calculate the bearing strength of the specimens tested in this study, then the average values of the ratio of $V_{n(test)}/V_{n(proposed)}$ for specimens SCB-ST and SCB-SB of 1.00 and 1.01, respectively, were obtained, with standard deviations of 0.09 and 0.11, respectively. As shown in Fig. 13, the predicted values from the proposed equations are in good agreement with the measure strengths.

6. Conclusions

The following conclusions were derived from the results of the experiments and analytical work carried out in this study on the bearing strength of connection between steel coupling beam and reinforced concrete shear wall:

1) In extracting the theoretical equation (7) for the bearing strength of connection between steel coupling beam and reinforced concrete shear wall, the assumption of a constant value of $c/l_e = 0.66$ is reasonable.
2) The length of the concrete compression zone below the embedded steel coupling beam is effectively constant, and is equal to about 72% of the embedded length of the steel coupling beam.
3) When calculating the bearing strength of a steel coupling beam section embedded in a shear wall, the PCI Code and other proposed models yield very conservative results. Therefore, from this study, the following equations are proposed to calculate the bearing strength of the connection between steel coupling beam and reinforced concrete shear wall

$$V_{n(proposed)} = f_b \beta_1 b l_e \left(\frac{0.58 - 0.22\beta_1}{0.88 + a/l_e} \right) + \frac{2(0.88 - a/l_e)\sum_{i=1}^{n} A_{si} f_{si}}{0.88 + a/l_e} \quad \text{(N)}$$

For a member without horizontal ties

$$f_b = 4.5\sqrt{f_{ck}} \left(\frac{t}{b} \right)^{0.55} \quad \text{(MPa)}$$

References

1. Gong, B. and Shahrooz B. M., "Concrete-Steel Composite Coupling Beams", *Journal of the Structural Division*, ASCE, Vol.127, No.6, 2001, pp.625~631.
2. Pauley, T. and Binney, J. R., "Diagonally Reinforced Coupling Beams of Shear Walls", *Shear in Reinforced Concrete: Publication No.42*, Amer. Concrete Inst., Detroit, USA, 1974, pp.579~598.
3. Shiu, K. N., Barney, G. B., Fiorato, A. E., and Corley, W. G, "Reversed Load Tests of Reinforced Concrete Coupling Beams", *Proceedings of the Central American Conf. on Earthquake Engineering*, El Salvador, 1978, pp.239~249.
4. Wan-Shin Park and Hyun-Do Yun., "Seismic behaviour of steel coupling beam linking reinforced concrete shear wall", *Journal of Engineering Structure*, 2005, Vol.27, No.7, pp.1024~1039.
5. *PCI Manual on Design of Connections for Precast Prestressed Concrete*, Prestressed Concrete Institute, Chicago, 1973, pp.25~38.
6. *PCI Design Handbook – Precast and Prestressed Concrete*, Prestressed Concrete Institute, Chicago, 1978, 370pp.
7. Kriz, L. B. and Raths, C. H., "Connection in Precast Concrete Structures–Shear strength of Column Heads", *Journal of Prestressed Concrete Institute*, Vol.8, No.6, December 1963, pp.45~75.
8. Williams, A., *The Bearing Capacity of Concrete Loaded Over a Limited Area*, Technical Report No. 526, Cement and Concrete Association, London, August 1979, pp.70~80
9. Mattock, A. H. and Gaafar, G. H., "Strength of Embedded Steel Sections as Brackets", *ACI Journal*, Vol.79, No.9, March-April 1982, pp.83~93.
10. Clarke, J. L. and Symmons, R. M., "*Test on Embedded Steel Billets for Precast Concrete Beam-Column Connection*, Technical Report No. 42. 523, Cement and Concrete Association, London, August 1978, pp.12~24.
11. Marcakis K. and Mitchell D., "Precast Concrete Connection with Embedded Steel Member", Journal of Prestressed Concrete Institute, Vol.25, No.4, July-August 1980. pp.86~116.
12. Shahrooz B. M., Remmetter M. A., Qin F., "Seismic Design and Performance of Composite Coupled Walls," *Journal of the Structural Division*, ASCE, Vol.119, No. 11, 1993, pp.3291~3309.
13. Harries, K. A., *Seismic Design and Retrofit of Coupled Walls using Structural Steel*, Department of Civil and Applied Mechanics, McGill University, Montreal, Canada, 1995.
14. ACI Committee 318, *Building Code Requirements for Structural Concrete and Commentary*, American Concrete Institute, Detroit, USA 2005, pp.105~110.
15. Kent, D. C. and Park, R., "Flexural Members with Confined Concrete", *Journal of the Structural Division*, ASCE, Vol.97, ST7, July 1971, pp.1969~1990.
16. Gong B., Shahrooz B. M., and Gillum A. J., *Cyclic Response of Composite Coupling Beams*, ACI Committee 335 Special Publication, 1997.
17. Gong B. and Shahrooz B. M., "Concrete – Steel Composite Coupling Beams", *Journal of Structural Engineering*, Vol.127, No.6, June 2001, pp.625~631.
18. Shahrooz B. M., Remmetter M. A., and Qin F., *Seismic Response of Composite Coupled Walls*, Composite Construction in Steel and Concrete II, ASCE, New York, N. Y., 1992, pp.428~441.
19. Hawkins, N. M., "The Shear strength of Concrete for Strip Loading," Magazine of Concrete Research (London), V. 22, No. 71, June 1970, Aug. 1979, pp.87~97.

Notation

a = distance from the concentrated load to the face of the column or shear wall(in mm)

A = coefficient in equation (14)

b = width of the embedded steel section(in mm)

b_{eff} = effective width of the concrete compression block (in mm)

c = length of compression zone below embedded steel section(in mm)

C_b = resultant concrete compressive force acting on top and at back of embedded steel section(in N)

C_f = resultant concrete compressive force acting below and at front of embedded steel section(in N)

e = lever arm of load applied to embedment(in mm)

f_b = concrete bearing stress (in MPa)

f_c = concrete stress (in MPa)

f_{ck} = specified concrete compressive strength(in MPa)

f_{cu} = concrete compressive strength measured on 150×300mm(6×12in.) cylinders(in MPa)

l_e = length of the embedment of steel coupling beam in concrete shear wall(in mm)

L = clear span of coupling beam(in mm)

l_{eff} = effective clear span of the coupling beam(in mm)

l_v = distance from concentrated load to the resultant compression force C_f (in mm)

n = exponent in Equations (14) and (15)

t = width of column or thickness of the shear wall(in mm)

V = concentrated load acting on the embedded section (in N)

V_n = nominal strength, i.e., value of load V at ultimate strain(ϕ=1.0) (in N)

β_1 = ratio of the depth equivalent rectangular stress distribution to the depth of flexural compression zone as specified in Section 10.2.7 of ACI 318-05

ε = concrete strain.

ε_b = strain in the concrete above the rear end of the embedded steel section.